MODELING AND SIMULATION OF TURBULENT NON-PREMIXED COMBUSTION IN CYLINDRICAL FURNACE

Ronchetti, Bernardo, bernronc@yahoo.com.br
Vielmo, Horácio A., vielmoh@mecanica.ufrgs.br
UFRGS, Mechanical Engineering Graduation Program. Rua Sarmento Leite, 425, 90050-170, Porto Alegre, RS

Abstract: *This work shows numerical solutions forexperimental cases from the literature. Simulations are made using different models for turbulent combustion of non-premixed gases. The final goal of the work is to determine the best way to simulate the phenomenon for the case of a cylindrical rotatory dryer. The studied cases show differences between turbulence models, reaction rate models and approaches in the radiation heat transfer. The main application discussed is the combustion of CH_4 with atmospheric air. The differential equations are solved through the Finite Volume Method. All geometries are discretized with a hexaedrical three-dimensional mesh. The numerical results are compared with experimental data and among each modeling alternative. Some results of the numerical simulations are different from the experimental results, but a discussion is made to reach the ideal configuration for modeling the furnace case according to physical behavior and accuracy to experimental data. The influence of the participant media in the radiative transfer in the chamber is shown in some of the cases and the importance of its modeling is discussed.*

Keywords*: Combustion modeling, non-premixed combustion, Finite Volume Method, combustion chamber, turbulence models.*

1. INTRODUCTION

Industrial furnaces are mainly designed in cylindrical geometries. One of the most used geometry in the mining processing industry is the rotary dryer, which is a machine used since the sand processing up to the complex process of kiln formation and clay foundry. This work is oriented to verify the main features in the commercial software, Cfx 10, analyzing theoretical points and technical capabilities in order to choose a methodology to develop a good assembly of burner and furnace in a stone rotary dryer.

The idea is to get as much information from test cases in free jet and swirled burner, appying in a new design concept for a burner in an existing rotary dryer. Actually almost all the burners in this derivation are oil burners, which are far away from getting environmental prorogation licenses due to the smoke and also exhaust gases, formed mainly from the very heavy compounds. The free jet furnace studied is the same chamber experimented by Garréton and Simonin (1995), also simulated by Silva (2005) in a 2D geometry and in non-structured mesh by Ronchetti et al. (2005). In all these works there is a very big concern about the model applied to the reaction rate which is basically a question of how much dynamics of the flow is bigger than the chemical demand of the reaction. The major parameter for the choice of the model to be used in the reaction rate calculation is the Damköler number (*Da*). This number relates the flow time scale and the chemical time scale. For high *Da* is interesting to use models that take into account the flow mixing since the reaction time is smaller. For low *Da,* the models that determine the reactions rate are strongly dependent of chemical kinetics of the reactions. When calculating reactive mixing flows with high and low Damköler's zones is better to use mixed models.

The objective now is with a 3D hexaedrical mesh, since the future burner does not have a symmetric geometry, to accomplish a good result and derive the theory to real furnace geometry. A swirled furnace is presented by Zhou (2003) with experimental and numerical results.

2. PROBLEM PRESENTATION

2.1. Chamber geometry-1

Figure 1 shows the case studied. It is a cylindrical chamber with fuel injection, CH_4 (methane), and oxidizer, atmospheric air (22% O_2, 78% N_2). They form of coaxial jets in the center of one of the extremes of the chamber. The chamber dimensions agree with Garréton and Simonin (1995), Silva et al. (2004), Magel et al. (1996) and Nieckele et al. (2001).

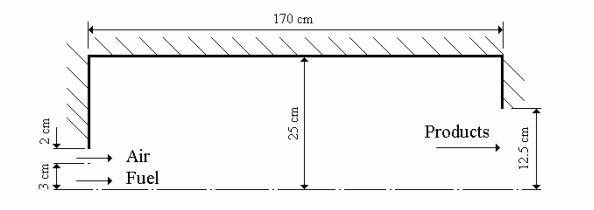

Figure 1. Combustion chamber geometry

The conditions for the air injection are 36.29 m/s, and 323.15 K. For the 7.71 m/s and 313.15 K. The turbulence intensity is 6% for the air, and turbulent length of 0.04 m. For the fuel the turbulent intensity is 1% and the turbulent length is 0.03 m. With these conditions and for atmospheric air with density 1.02 kg/m³ and methane 0.649 kg/m³, the chamber develops approximately 400 kW of power. The mass flows are 0.0125 kg/s of CH_4 and 0.186 kg/s of air, in agreement with Garréton and Simonin (1995). The wall boundary condition is prescribed temperature of 393 K. The study case is a god case because it's the geometry employed by many burners in the industry. It's also possible to obtain information for bigger systems as drying furnaces, rotary dryers, incinerators and steam generators.

2.2 Domain discretization

The domain is discretized in hexaedrons which have a better capability to save computational effort and better accuracy results. Three meshes (Fig.2) are used in order to analyse the effects in the flow and also in the thermal field. The first one being formed by the chamber only (a), and two others where there is also assembled the exhaust gases exit duct ((b) 600mm extent and (c) 1200mm extent). It is verified the effect of local temperature condition in the radiation calculation, since there is the buoyancy effect, that's calculated.

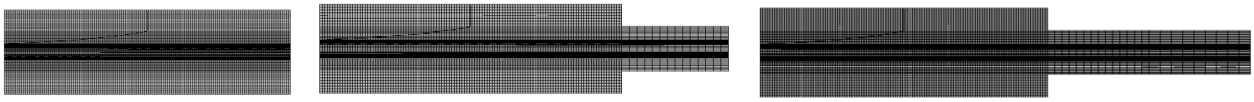

(a) 784825 nodes (b)259302 nodes (c)270399 nodes

Figure 2. Meshes used in the calculation of the furnace

3. MATHEMATICAL FORMULATION

It's considered that the heat transfers has already happened reaching steady state. The heat transfer happens from the hot gases (products of the combustion processes) to the ambient. The objective of the work is to show the distribution of temperatures and gas concentrations. They are applied different turbulence models: $k-\varepsilon$, $k-\omega$, BSL, SST, and Reynolds Stress Transport Models, SSG. The radiative heat transfer is calculated through the DTRM - Discrete Transfer Radiation Model which solve for the intensity of radiation, *I*, along rays leaving from the boundaries. After it integrates *I* over solid angle at discrete points to find the incident radiation and the radiant heat flux. Using the hypothesis of homogeneity to extend the solution to the whole dominium, it's considered gray gas with isotropic scattering of coefficient 0.5 (m^{-1}).

3.1. Phenomenon equations

The equations to solve in the simulation of the combustion phenomenon in steady state are mass conservation, momentum conservation, energy conservation and chemical species conservation, as follows:

3.1.1 Mass conservation

For the stationary case, $\frac{\partial \rho}{\partial t} = 0$, Eq.(1) shows the mass balance.

$$\nabla \bullet (\rho U) = 0 \qquad (1)$$

in which, U is the Reynolds average velocity, and ρ is the density.

3.1.2 Momentum equation

Equation (2) shows the momentum balance in a stationary situation, $\frac{\partial \rho U}{\partial t} = 0$ and no momentum source, $S_M = 0$.

$$\nabla \bullet (\rho U \otimes U) = \nabla \bullet \left(- p\delta + \mu\left(\nabla U + (\nabla U)^T\right)\right) \tag{2}$$

Equation (3) shows the momentum balance as Eq.(2) but in a Reynolds averaged form

$$\nabla \bullet (\rho U \otimes U) = -\nabla p' + \nabla \bullet \left(\mu_{eff}\left(\nabla U + (\nabla U)^T\right)\right) \tag{3}$$

where μ_{eff} is the effective, adding the dynamic viscosity and the turbulent , μ_t, computed or from the standard $k-\varepsilon$ model by $\mu_t = C_\mu \rho k^2 / \varepsilon$ or by any other model, $p' = \overline{p} - \left(2/3\right)k$ represents the modified pressure, $\overline{p}$ is the average pressure.

3.1.3. Energy conservation

For the energy transport due to the flow inside the chamber, neglecting the energy transport due to the diffusion of each species ($Le = 1$), in stationary situation, $\frac{\partial \rho h_{tot}}{\partial t} = 0$ and $\frac{\partial p}{\partial t} = 0$, Eq. (4):

$$\nabla \bullet (\rho U h_{tot}) = \nabla \bullet (\lambda \nabla T) + S_E \tag{4}$$

where h_{tot} is the average total enthalpy of the mixture, λ c_p is is the thermal conductivity of the mixture, defined as $\lambda = \sum_\alpha f_\alpha \lambda_\alpha$, where λ_α is the thermal conductivity of the α-th chemical species, T is the average temperature, S_E is the source term due to the heat transfer by radiation and chemical species formation, Eq.(5):

$$S_E = S_{rad} + \sum_\alpha \left[\frac{h_\alpha^0}{\overline{MM}_\alpha} + \int_{\overline{T}_{ref,\alpha}}^{\overline{T}} c_{p,\alpha} d\overline{T}\right]\overline{R_\alpha} \tag{5}$$

h_α^0 and $\overline{T}_{ref,\alpha}$ terms are the enthalpy of formation and the reference temperature of the α-th chemical species. $\overline{MM}_\alpha$ is the molecular mass of the α-th chemical species. The solution of S_{rad} is made using DTRM (CFX, 2002) in some of the cases. The component source term is linearised to achieve robust convergence and prevent negative values.

3.1.4. Turbulence Models

Two equations turbulence models are largely used, they offer a commitment between numerical effort and computer accuracy. The turbulent viscosity is modeled with the product of the turbulent velocity and the length turbulent scale. In the two-equation models the turbulent velocity scale is estimated from the solution of these transport equations. The turbulent length is estimated of the two properties of the turbulent flow field, usually the turbulent kinetic energy and its dissipation. The dissipation rate is supplied by the solution of these transport equations. When observing trough time scales bigger than the real time scales of the turbulent fluctuations, it's possible to say that the turbulent flow shows average characteristics, with an additional time variant component.

3.1.4.1. $k-\varepsilon$ model

The models $k-\varepsilon$ and also $k-\omega$ use the hypothesis of diffusion in the gradient to relate the Reynolds tensions to the average velocity and the turbulent viscosity. Kinetic energy conservation k and its dissipation ε are given by Eq. (6) and Eq. (7)

$$\nabla \bullet (\rho U k) = \nabla \bullet \left[\left(\mu + \frac{\mu_t}{\sigma_k}\right)\nabla k\right] + P_k - \rho\varepsilon \tag{6}$$

$$\nabla \bullet (\rho U \varepsilon) = \nabla \bullet \left[\left(\mu + \frac{\mu_t}{\sigma_\varepsilon} \right) \nabla \varepsilon \right] + \frac{\varepsilon}{k} (C_{\varepsilon 1} P_k - C_{\varepsilon 2} \rho \varepsilon) \tag{7}$$

where $C_{\varepsilon 1}$ and $C_{\varepsilon 2}$ are constants defined experimentally and characteristics of the turbulence model, σ_k and σ_ε represent the respective Prandtl numbers of the kinetic energy and its dissipation, and P_k the production or dissipation of the kinetic turbulent energy, accounting the buoyancy effect, defined with Eq. (8).

$$P_k = \mu_t \nabla U \bullet \left(\nabla U + \nabla U^T \right) - \frac{2}{3} \nabla \bullet U (3\mu_t \nabla \bullet U + \rho k) + \left(- \frac{\mu_t}{\mathrm{Pr}_t} g \bullet \nabla \rho \right) \tag{8}$$

3.1.4.2. $k - \omega$ model

One of the advantages of the formulation is the treatment near the wall for low *Re* numbers. The model does not involve complex functions of damping, needed into the $k - \varepsilon$ model. The model $k - \omega$ assumes that the turbulent viscosity is related to the kinetic turbulent energy by Eq. (9).

$$\mu_t = \rho \frac{k}{\omega} \tag{9}$$

The model solve two transport equations, one for kinetic energy, *k* and one for the turbulent frequency, ω. The stress tensor is calculated by the concept of turbulent viscosity, Wilcox (2000). The kinetic energy conservation equation is given by Eq. (10) and turbulent frequency by Eq.(11)

$$\nabla \bullet (\rho U k) = \nabla \bullet \left[\left(\mu + \frac{\mu_t}{\sigma_k} \right) \nabla k \right] + P_k - \beta' \rho k \omega \tag{10}$$

$$\nabla \bullet (\rho U \omega) = \nabla \bullet \left[\left(\mu + \frac{\mu_t}{\sigma_\omega} \right) \nabla \omega \right] + \alpha \frac{\omega}{k} P_k - \beta \rho \omega^2 \tag{11}$$

In addition to the independent variables, density, velocity vector, there are the quantities that come from the solution of the Navier-Stokes equations. P_k is the production of the turbulence rate, which is calculated for Eq. (8). The constants of the models are $\beta' = 0.09$, $\alpha = 5/9$, $\beta = 0.075$, $\sigma_k = 2$, $\sigma_\omega = 2$.

To avoid kinetic energy increase in the stagnation regions, a limiter (Eq. (12)) to the production term is introduced into the equations.

$$\tilde{P}_k = \min(P_k, c_{\lim} \varepsilon), \; c_{\lim} \varepsilon = 10 \tag{12}$$

3.1.4.3. BSL model

A disadvantage of the $k - \omega$ model is its high sensibility to effects of shear jets, free stream. So there is a possible combination between $k - \omega$, near wall, e $k - \varepsilon$ in outer region. The classic $k - \omega$ model from Wilcox Eq.(10) and Eq. (11) is multiplied by a combination function F_1 (Eq.(15)), Eq. (13)

$$\nabla \bullet (\rho U k) = \nabla \bullet \left(\left(\mu + \frac{\mu_t}{\sigma_k} \right) \vec{\nabla} k \right) + (1 - F_1) 2\rho \frac{1}{\sigma_{\omega 2} \omega} \nabla k \nabla \omega + \alpha_3 \frac{\omega}{k} P_k - \beta' \rho \omega^2 \tag{13}$$

And the $k - \varepsilon$ transformed model by $1 - F_1$, using Eq. (5). The function F_1 is 1 near the wall and zero at the boundary layer. In exterior and the limit of the boundary layer the $k - \varepsilon$ model begins to be used again. The constants of the BSL model are in Table 1

Table 1 – Constants used in $k-\varepsilon$ model.

β'	α_1	β_1	σ_{k1}	$\sigma_{\omega 1}$	α_2	β_2	σ_{k2}	$\sigma_{\omega 2}$
0.09	5/9	0.075	2	2	0.44	0.0828	1	1/0.856

3.1.4.4. SST model

SST model is based in $k-\omega$ model and brings good approximation for the cases of de-attachment of boundary layer and shear free layers, cause it accounts the effect of the Reynolds stress tensor. There could be a super estimative if the turbulent viscosity, to avoid it there can be installed a maximum acceptable value in the process, Eq. (14)

$$v_t = \frac{\alpha_1 k}{\max(\alpha_1 \omega, SF_2)} \tag{14}$$

α_1 is a constant and F_2 is a combination function, Eq. (18), similar to the BSL model. The formulation of this function is based in the distance from the nearest surface and the variables of the flow.

$$F_1 = \tanh\left(\arg_1^4\right) \tag{15}$$

$$\arg_1 = \min\left(\max\left(\frac{\sqrt{k}}{\beta' \omega y}, \frac{500v}{y^2 \omega} \right), \frac{4\rho k}{CD_{kw} \sigma_{\omega 2} y^2} \right) \tag{16}$$

$$CD_{k\omega} = \max\left(2\rho \frac{1}{\sigma_{\omega 2} \omega} \nabla k \nabla \omega, 1\times 10^{-10} \right) \tag{17}$$

where y is the distance to the nearest surface.

$$F_2 = \tanh\left(\arg_2^4\right) \tag{18}$$

$$\arg_2 = \max\left(\frac{\sqrt{k}}{\beta' \omega y}, \frac{500v}{y^2 \omega} \right) \tag{19}$$

The constants are the same used in BSL model.

3.1.4.5. Reynolds Transport Model - SSG

These models do not use the hypothesis of turbulent viscosity, but solve an equation for the transport of the Reynolds stresses in the fluid. The exact production term and anisotropies in the stresses suggest that these models should be used in complex flows, however some works showed that in some cases it do not overcome the two equation models, thanks to its computational cost.

There is a solution using the SSG (Speziale, 1991), in the work and the model has a difference from other models thanks to the constants used in the modeling of the Reynolds stress tensor and the correlation of pressure and fluctuations, that is quadratic. Table 2 shows the constants used in the SSG model.

Table 2 – Constants used in SSG model.

$C_{\mu RS}$	s_{eRS}	c_S	$c_{\varepsilon 1}$	c_{e2}	C_{s1}	C_{s2}	C_{r1}	C_{r2}	C_{r3}	C_{r4}	C_{r5}
0.1	1.36	0.22	1.45	1.83	1.7	-1.05	0.9	0.8	0.65	0.625	0.2

3.1.5. Chemical species conservation

A conservation equation is required for all the components presents at the chemical reaction, except for the nitrogen. In this way, assuming a Lewis number of 1.0, one obtains the following conservation equation of the α–th chemical species, Eq.(20):

$$\nabla_i \bullet \left(U_i \rho f_\alpha\right) = \nabla\left(\left(\rho D + \frac{\mu_t}{Sc_t}\right)\nabla_i f_\alpha\right) + \overline{R_\alpha} \tag{20}$$

where D is the mass diffusivity, Sc_t is the Schmidt number, $\overline{f_\alpha}$ is the average mass fraction of the α–th chemical species of the mixture, and $\overline{R_\alpha}$ is the average volumetric rate of the formation or destruction of the α–th chemical species. This term is computed as the summation of all volumetric rates of formation or destruction in all chemical reactions k in which α is present, $\overline{R_{\alpha,k}}$. The source term is directly related to the reaction rate R_k, Eq. (21).

$$\overline{R_\alpha} = \overline{MM}_\alpha \sum_{k=1}^{K}\left(\eta''_{\alpha,k} - \eta'_{\alpha,k}\right)\overline{R_{\alpha,k}} \tag{21}$$

where $\eta''_{\alpha,k}$ and $\eta'_{\alpha,k}$ are the backward and the forward stoichiometric coefficient of the α-th chemical species that are present in the k-reactions.

3.1.5.1 Reaction rate models

The finite rate chemistry model is based on the Arrhenius law, where the average reaction rate is calculated by the Eq. (22)

$$\overline{R_{\alpha,k}} = \left(A_k \overline{T}^{\beta_k} e^{\left(-\frac{E_k}{R\overline{T}}\right)} \prod_{\alpha=A,B,\ldots}^{N_C} [\alpha]^{\gamma'_{\alpha,k}} - A_k T^{\beta_k} e^{\left(-\frac{E_k}{R\overline{T}}\right)} \prod_{\alpha=A,B,\ldots}^{N_C} [\alpha]^{\gamma''_{\alpha,k}}\right) \tag{22}$$

where $\overline{R_{\alpha,k}}$ is the progress rate of the reaction k of the α–th chemical species, E_k is the activation energy, β is the dimensionless exponent of the temperature, and A_k is the pre-exponential factor that follow dimensions consistent with the unities of $R_{\alpha,k}$, $\gamma_{\alpha,k}$ is the exponent of the α–th chemical species into the reaction k and $[\alpha]$ is the molar concentration of the component α, where the subscript of $\gamma_{\alpha,k}$ identifies the direction of the reaction (´´) reactants-products and (´) products-reactants.

The Eddy Breakup model is based in the concept that the chemical reaction is fast compared to the chemical kinetic. In turbulent flows this characteristic time is determined by the properties of the turbulent structures (eddies). The mixing time between the components of the flow is proportional to the relation between kinetic energy k and the kinetic energy dissipation ε, Wilcox (2002). As a result the reaction rate is proportional to the inverse of this relation, Eq. (23) and Eq. (24).

$$\overline{R_{\alpha,k}} = A\frac{\varepsilon}{k}\min\left(\frac{[\alpha]}{\eta'_{\alpha,k}}\right) \tag{23}$$

$$\overline{R_{\alpha,k}} = AB\frac{\varepsilon}{k}\left(\frac{\sum_P [\alpha]\overline{MM}_\alpha}{\sum_P \eta''_{\alpha,k}\overline{MM}_\alpha}\right) \tag{24}$$

Where in the equation, A and B are dimensionless empirical coefficients. In the Eddy-Breakup model (EBU) it's chosen the smallest reaction rate calculated. Equation (15) the limited rate of the products and it's not used in multiple steps reactions. It's widely employed in combustion simulation a model coupling the reaction rate calculation by the Arrhenius and the EBU model. For modeling the chemical reaction in the present problem it's used the results of two reactions, Eq. (25) and Eq. (26).

$$CH_4 + 1,5O_2 \rightarrow CO_2 + 2H_2O \tag{25}$$

$$CO + 0,5O_2 \rightarrow CO_2 \tag{26}$$

The parameters used into the reactions are given by Tab. 3.

Table 3 – Adopted parameters for the reaction rate calculation.

Reaction	A_k	E_k	β_k	$\gamma_{CH_4,k}$	$\gamma_{O_2,k}$	$\gamma_{CO_4,k}$	$\gamma_{H_2O,k}m$	$\gamma_{CO,k}$
1	$1.5\left(1/s\right)$	$125400\left(J/mol\right)$	0	-0.3	1.3	1	2	-
2	$10^{14.5\left(1/mol^{0.75}m^{4.5}s\right)}$	$167200\left(J/mol\right)$	0	-	0.25	1	-	1

The dimensions of the pre-exponential factor should agree to get $\overline{R_{\alpha,k}}$ in $\left(mol/s\right)$ and the orders of the reaction γ give the result of the difference between A_k of the two reactions. For the value of the dimensionless empirical coefficients A and B of the EBU it is used the values 4 and 0.5, (Fluent Inc., 1997).

4.RESULTS AND DISCUSSION

The furnace experimented by Garrèton and Simonin was an object to develop a good model to calculate the narrow flame form of a burner in a furnace. The configuration of free jet burner is quite common when operating burners in the narrow flame form.

4.1. Turbulence models comparison

From bibliography it's possible to identify a major presence of two-equation models in solutions of cylindrical chambers. In this case specifically there are some models that are known to do not give an accurate answer in simulating the flow. Observing the streamlines of the flow there is a certain similarity but when evaluating the velocity values near wall, where there is the reattachment of the flow, Fig.3, it's possible to see that two equation models are a low computational cost solution that reaches a good result. Silva (2005) and Nieckele et al. (2001) used a two-equation model with a good approximation of the results from Garrèton et Simonin (1995), this is a parameter to evaluate which model approaches better the solution.

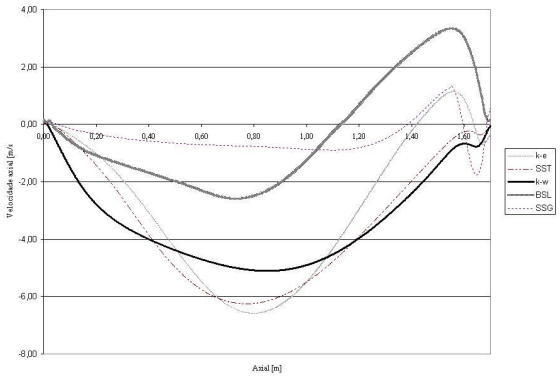

Figure 3. Behaviour of different turbulent models in the wall of the furnace.

The two equations models show good behavior, comparing all models computing in a P4, 2.4 GHz, personal computer with 2 Gb in RAM and a mesh with 727000 nodes without radiation calculation. Table 4 shows the time comparison.

Table 4. Time demanded by each turbulence model.

MODEL	k-e	SST	BSL	SSG	k-w
Time [s]	8.7e4	7.61e4	5.31e4	1.36e4	5.96e4

The comparison for the situations modeled is made using the profiles of temperature and concentration of chemical species. Using different manners for calculating the kinetic energy and its dissipation, according to the characteristics of the model, there will be a significant difference in the calculated mixing time, therefore should be different Damkholer numbers and also reaction rates in regions dominated by the physical mixture of the species. Only the mesh of 724825 is considered in the comparison, since the exhaust piping won't have any effect in this aspect, and a numerical experience showed good results with this grid configuration. Figure 4 shows the temperature profiles along the chamber.

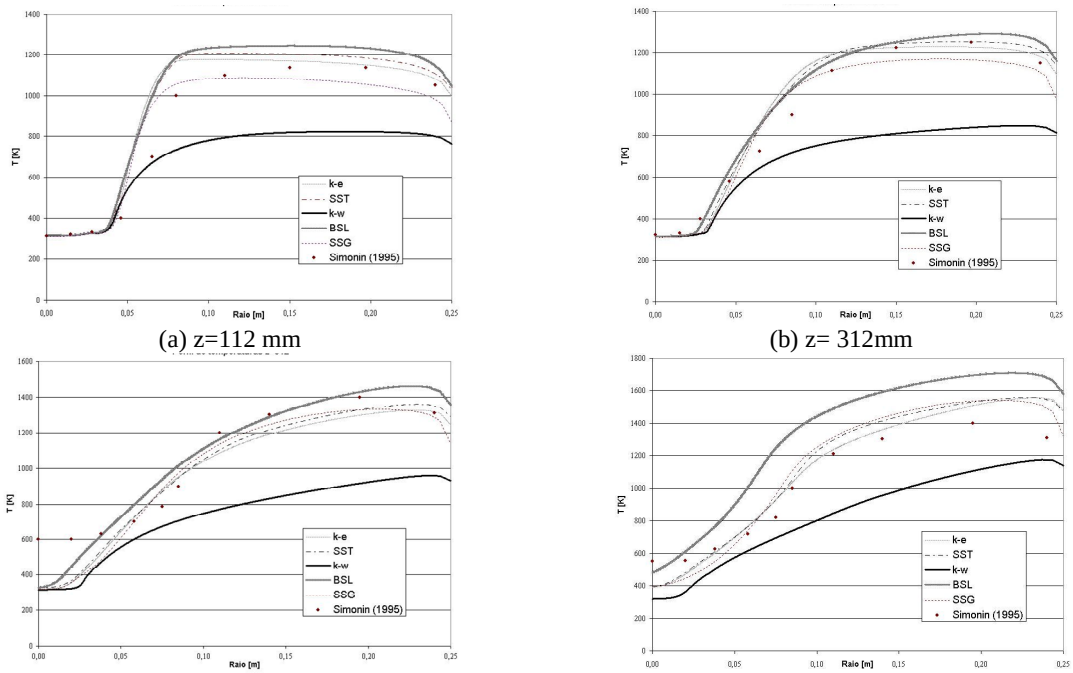

(a) z=112 mm (b) z= 312mm

© z=612mm (d)z=912mm

Figure 4. Temperature profiles along the chamber.

Analyzing the profiles it's possible to see that the models showed a quite difference exposed in the experimental results after the middle of the chamber. The model that shows better reliability according to the results was k-e, SST and BSL. To evaluate the reaction rate effect in the chemical species transport with the different models Fig. (5) shows the profiles of CO2 mass fraction in the two most significant lengths of the chamber, 312 mm and 912 mm.

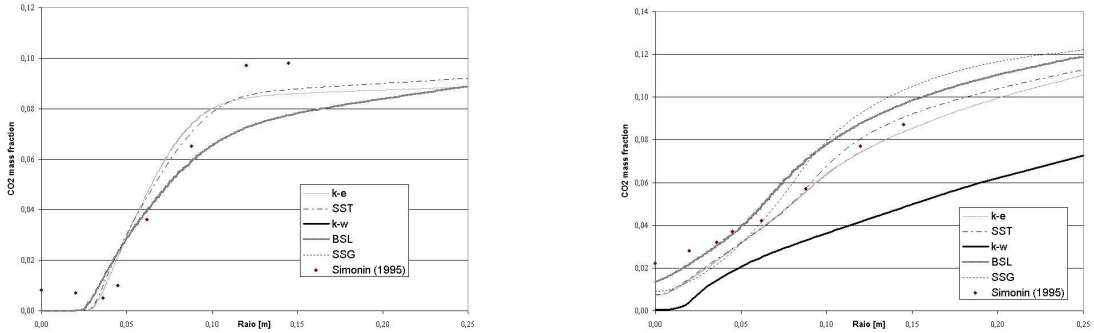

(a) z=312mm (b) z=912mm

Figure 5. CO_2 mass fraction profiles.

All models show good physical behavior except the original k-w model, its formulation dedicated to flow near surfaces is quite a tool for small chambers but here shows quite a difficulty for solving this case. The SSG model show good physical behavior but there's a bigger computational cost in order to use it.

Although the BSL model shows good physical behavior in the flow, there's a point to observe temperature and concentration profile, cause there is always a super estimation, so the k-e would be a better solution for the case, even

SST that shows good practical results in concentration profiles, but bad results in flow solution. The results were physically accepted to denote the same behavior of the experimental results, but there are still numerical differences due to the fact that there's no radiation solved and also buoyancy.

4.2. Geometry furnace effect in the solution

With turbulence model chosen and knowledge of how much computational cost it expends, a new calculation of the chamber is made to see the effect of buoyancy effects and also boundary conditions.

4.2.1 Furnace without exhaust extension.

There's not much modification in temperature field but chemical species transport and reaction are better accomplished as seen by a further section of the chamber (z=912 mm), showing better behavior of chemical species transport and a dependency in the boundary condition of the outlet, Fig.(6).

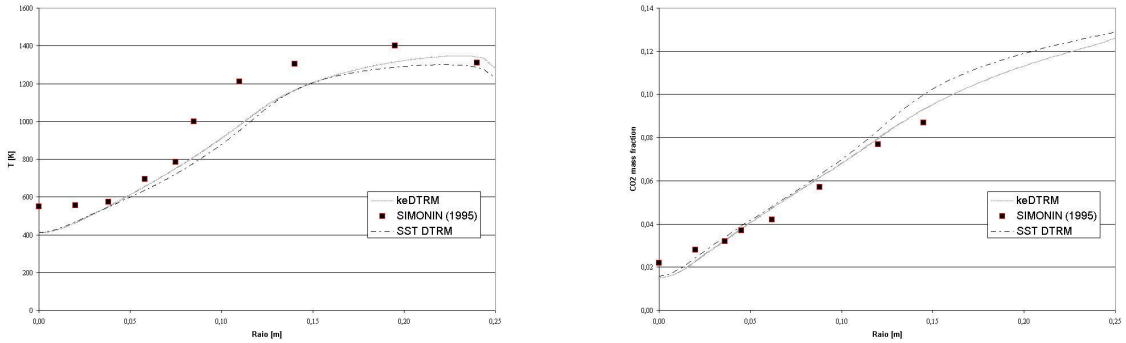

(a) (b)

Figure 6. (a) Temperature profiles (b) Concentration profiles.

The use of buoyancy, radiation and turbulence model in a refined mesh shows better results when compared with the simple turbulence model and no radiation transfer calculation showed above. There's a better reaction rate calculation exposed but there is a temperature distribution problem when comparing the profiles. K-e shows a quite better liability with experimental data and also SST had a reattachment length at 100% of the chamber, as said before, which do not suppose its use.

4.2.2 Furnace with exhaust extension of 600 mm.

Another test case, now coarsening the mesh adding also an extension of the exhaust pipe of the chamber shows better accordance with experimental data, in the temperature field, Fig.(7).

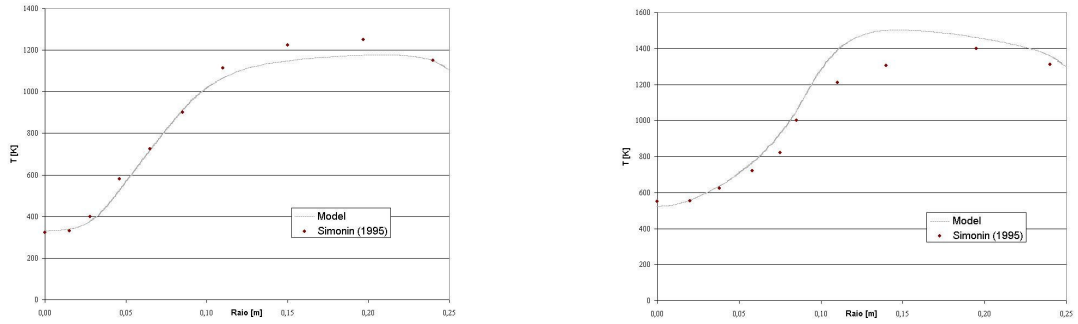

(a) z=312 mm (b) z=912 mm

Figure 7. Temperature profiles of the chamber

The concentration of chemical species is already well defined as shown in the previous section, the objective is to see how important is the boundary condition in the radiation calculation.

4.2.3 Furnace with exhaust extension of 1200 mm.

The solution shows that there is a high interference of the boundary condition of the outlet of the chamber in the temperature field. The final model adopted show differences of maximum 100 [K] near the fuel inlet and the chemical species concentration are in values very close to the experimental, as shown in Fig.(8).

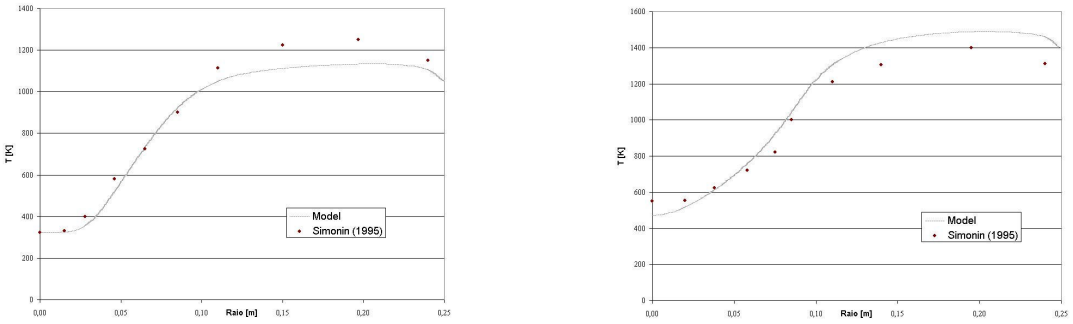

(a) z=312 mm (b) z= 912 mm

Figure 8. Temperature profiles

5. CONCLUSION

As a conclusion for the study of a furnace with this configuration the final model with exhaust pipe coupled to the mesh, radiation and buoyancy solved it is possible to achieve quality results in order to guide a burner design. The $k-\varepsilon$ model shows good performance for the prediction in the chamber, but the BSL model will be again reviewed due to its good behavior in predicting the jet.

Zhou (2003) shows a simulation of a chamber with a swirl burner, which is the case of burners operating in the wide flame form and different swirls numbers. From the comparison of the simulated data from Zhou and its experimental data, it is possible to achieve a model that can predict the behavior of a burner in wide flame form in a rotary dryer. As a result of this work, it will be developed of a dual burner using natural gas and that has the capability of flame form variation.

6. REFERENCES

Cfx Inc., 2002. “CFX user’s guide”, CFX, Waterloo.

Eaton, A. M., Smoot,L.D., 1999, “Components, Formulations, Solutions, Evaluation, and application of comprehensive combustion models”, Progress in Energy and Combustion Science, Vol.25, pp.387-436.

Garréton, D., Simonin, O., 1995, “Aerodynamics and steady state combustion chamber and furnaces”, Ecoftac Bulletin, pp. 29-38.

Glassman, I., 1977, “Combustion”, Academic Press, London.

Fluent Inc., 1997. “Fluent user’s guide”, Fluent Incorporated, New Hampshire.

Magel, H.C., Schnell, U., Hein, K.R.G., 1996-a. “Modeling of hydrocarbon and nitrogen chemistry in turbulent combustor flows using detailed reactions mechanisms”, 3rd Workshop on Modeling of Chemical Reaction Systems, Heidelberg.

Magel, H.C., Schnell, U., Hein, K.R.G., 1996-b. “Simulation of detailed chemistry in a turbulent combustor flow”. Twenty-Sixth Symposium (International) on Combustion/The Combustion Institute, pp.67-74.

Nieckele, A.O., Naccache, M.F., Gomes, M.S.P., Carneiro, J.E. and Serfaty, R., 2001. “Evaluation of models for combustion processes in a cylindrical furnace”, ASME-IMECE, International Conference of Mechanical Engineering, New York

Ronchetti, B., Silca, C.V.,Vielmo, H. A., 2005, “Simulation of Combustion in Cylindrical Chamber”, Proceedings of the 18th Brazilian Congress of Mechanical Engineering, Ouro Preto, Brazil, COBEM2005-1541.

Silva, C. V. da, 2005, “Numerical simulation of turbulent combustion of natural gas in cylinrical chamber”, Doctoral Dissertation, UFRGS, Porto Alegre, Brazil.

Zhou, L.X.,et al., 2003, “Simulation of swirling combustion and NO formation usinh a USM turbulence-chemistry model”, Fuel, Vol. 82, pp. 1579-1586.

5. RESPONSIBILITY NOTICE

The authors are the only responsible for the printed material included in this paper.